Scanning Microscopy

Volume 2 | Number 2 Article 14

2-23-1988

# Low Energy Cathodoluminescence Spectroscopy of Semiconductor Interfaces

L. J. Brillson
*Xerox Webster Research Center*

R. E. Viturro
*Xerox Webster Research Center*

Follow this and additional works at: https://digitalcommons.usu.edu/microscopy

Part of the Life Sciences Commons

## Recommended Citation

Brillson, L. J. and Viturro, R. E. (1988) "Low Energy Cathodoluminescence Spectroscopy of Semiconductor Interfaces," *Scanning Microscopy*: Vol. 2 : No. 2 , Article 14.
Available at: https://digitalcommons.usu.edu/microscopy/vol2/iss2/14

This Article is brought to you for free and open access by the Western Dairy Center at DigitalCommons@USU. It has been accepted for inclusion in Scanning Microscopy by an authorized administrator of DigitalCommons@USU. For more information, please contact digitalcommons@usu.edu.

Scanning Microscopy, Vol. 2, No. 2, 1988 (Pages 789-799) 0891-7035/88$3.00+.00
Scanning Microscopy International, Chicago (AMF O'Hare), IL 60666 USA

# LOW ENERGY CATHODOLUMINESCENCE SPECTROSCOPY OF SEMICONDUCTOR INTERFACES

L. J. Brillson* and R. E. Viturro

Xerox Webster Research Center
800 Phillips Rd 114/41D
Webster, NY 14580

(Received for publication March 03, 1987, and in revised form February 23, 1988)

## Abstract

Low energy cathodoluminescence spectroscopy (CLS) is a powerful new technique for characterizing the electronic structure of "buried" semiconductor interfaces. This extension of a more conventional electron microscopy technique provides information on localized states, deep level defects, and band structure of new compounds at interfaces below the free solid surface. From the energy dependence of spectral features, one can distinguish interface versus bulk state emission and assess the relative spatial distribution of states below the free surface. Low energy CLS reveals process changes in the electronic structure of semiconductor interfaces due to metallization, laser annealing, and thermal desorption. Spectral features of metal-semiconductor interfaces uncovered by CLS also provide a new perspective on physical mechanisms of Schottky barrier formation.

**Key words:** Cathodoluminescence, Metal-Semiconductor Interface, Schottky Barrier Formation, Interface States, Defects, Depth-Dose, Electron Range, Semiconductors, InP, GaAs, CdS, Dead Layer, Deep Levels, Interface Reaction.

**Address for correspondence:**
Leonard J. Brillson
Xerox Webster Research Center
800 Phillips Rd 114/41D
Webster, NY 14580
Phone No.: (716) 422-6468

## Introduction

Cathodoluminescence spectroscopy (CLS) and cathodoluminescence mapping are well-known electron microscopy techniques for studying electronic structure and free carrier recombination of bulk semiconductors.[53] Combined with photoluminescence spectroscopy, these techniques have been useful in evaluating semiconductor growth quality and its variations near grain boundaries, growth artifacts, and other microscopic imperfections of the crystalline material. See, for example references 28, 29 and 31. Included are gauges of minority carrier lifetime[10,45], diffusion length[34,50], carrier concentration,[10] and defect segregation.[30] Furthermore, CLS provides a measure of spatially-localized band structure and deep levels in modulated semiconductor structures.[17,30]

In the last several years, researchers have begun using a low energy extension of CLS to study semiconductor surfaces and "buried" metal-semiconductor interfaces. Motivating this work has been the need to probe electronic structure of metal-semiconductor junctions at metallic coverages, in order to elucidate the fundamental mechanisms involved in Schottky barrier formation. Whereas conventional surface science techniques have provided considerable information on the initial stages of contact rectification[4], they are by definition of little value in studying the "buried" interface. To investigate such interfaces, one requires the facility to probe tens of monolayers below the free surface without sampling primarily the characteristics of the bulk semiconductor. Researchers have observed clear evidence for electronic states localized near surfaces and interfaces, including metal-induced deep levels, defect levels, and band structure of localized compound layers. The ability to observe such features are due in large part to the surprisingly high near-surface sensitivity of low energy CLS. Furthermore, merely by increasing the incident electron energy, one can obtain information from the sub-surface region and the bulk material, thereby providing a means to compare near-surface and bulk phenomena directly.

CLS results for semiconductor surfaces show dramatic differences across the same surface depending on chemical composition, roughness or bulk defect concentration. CLS results for metal films on clean semiconductor surfaces reveal discrete

emission to or from states deep within the semiconductor band gap which depend on the specific metallization and/or thermal treatment employed. Hence low energy CLS represents a unique new tool for identifying the physical mechanisms which contribute to formation of interface electronic structure and in particular the barriers to electrical charge transport.

In the following sections, we present a description of the experimental technique, the dependence of excitation depth on incident voltage in the low energy regime, CLS studies of semiconductor surfaces, CLS studies of metal-induced surface states, CLS studies of thermally-processed interfaces, implications for understanding Schottky barrier formation, and future applications.

## The Low Energy Cathodoluminescence Spectroscopy Technique

Figure 1 illustrates schematically the low energy cathodoluminescence experiment.[6] In addition to an ultrahigh vacuum (UHV) chamber for preparing and maintaining clean and chemically-modified semiconductor surfaces, one requires a low energy (300-3000 eV) glancing incidence electron gun, a monochromator and photon detector with near-infrared sensitivity, and suitable photon collection optics. The latter consists of a quartz lens to collect the luminescence signal excited by the glancing incidence electron beam, and a sapphire vacuum viewport to pass the light through to a Leiss double prism monochromator. Both prism and grating monochromators are available which span the spectral range from the infrared to the near-ultraviolet. However, grating monochromators typically require a change of gratings over a broad spectral range as well as filters to cut out second-order diffraction.

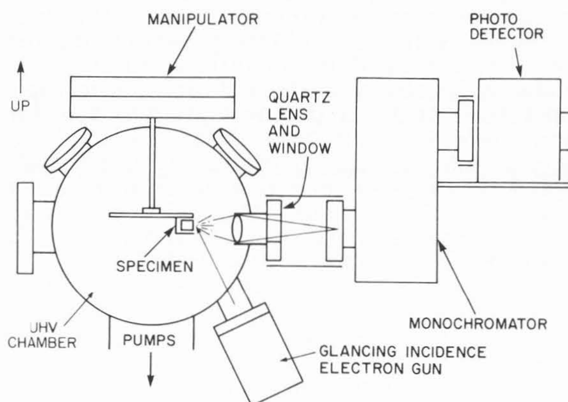


Fig. 1. Schematic experimental arrangement for cathodoluminescence spectroscopy under ultrahigh vacuum conditions.

A liquid-nitrogen-cooled S-1 photomultiplier is a common choice for sensitive light detection from the near infrared to the ultraviolet. Ge, InSb, and PbS detectors are available for detection at longer infrared wavelengths, although their detectivities are lower and are usable only over rather limited wavelength ranges. Lock-in techniques provide some improvement in signal-to-noise ratio for all of these detectors and are especially useful in removing the infrared background due to the glow of electron gun filament reflecting off the specimen. The combination of CLS with UHV conditions provides an additional benefit: by varying surface conditions in a controllable and verifiable fashion, it is possible to isolate and identify electronic features related to the surface only.

## Energy Dependence of Excitation Depth

The success of CLS in detecting semiconductor interface and even surface features derives mainly from the small penetration depths of the low energy incident electron beam. Whereas electron microscopes in the 100 keV to MeV energy range typically excite luminescence over depths of tens or hundreds of microns, electron beams of several hundred to several thousand eV produce luminescence from a depth of only fractions of a micron. The glancing incidence (ca. 30°) of the electron beam on the specimen provides an additional decrease in the penetration depth of the secondary electron cascade.[22,23] Hence luminescence is observable from energy levels located at "buried" interfaces many tens of monolayers below the free surface without probing appreciable depths of the underlying substrate.

The metal film on semiconductor structure serves to enhance the interface signal relative to the substrates as well. The metal overlayer serves to reduce electron penetration into the semiconductor without contributing to the luminescence. (Nevertheless CL emission from the semiconductor surface without any metal overlayer is also observable). Likewise the band bending within the semiconductor surface space charge region can separate electron-hole pairs generated by the electron beam, thereby reducing the probability for luminescence.[51] This "dead layer" reduces luminescence from the semiconductor substrate which could otherwise dominate a small interface signal. Band bending can also enhance the interface luminescence by raising the joint density of electron and hole states near the semiconductor surface. Thus for upward (n-type) band bending, excited holes tend to accumulate at the semiconductor surface, thereby enhancing the probability for optical transitions to the valence band at the interface.

Unfortunately, quantitative data is not available for the excitation depths of the electrons employed in low energy CLS. Instead we must estimate the maximum electron range and the depth of maximum energy loss (e.g., maximum electron-hole pair creation) from expressions derived for higher kinetic energies.

Everhart and Hoff [8] have obtained a universal range-energy relation which incorporates the average atomic weight A, average atomic number Z, and the density of the target material. The maximum range $R_B$ for a kinetic energy E is given by[37]

$$R_B' = K\int_0^{\zeta(E_o)} \zeta d\zeta/d(ln\zeta)\ gm/cm^2 \quad (1)$$

$$\zeta = 1.1658\ E/I \quad (2)$$

where

$$K = 9.4 \times 10^{-12} I^2 (A/Z)\ gm/cm^2 \quad (3)$$

with the "mean excitation energy"

$$I = (9.76 + 58.8Z^{-1.19})\ Z\ eV \quad (4)$$

for A in grams and I in eV

$$R_B = R_B'/K \quad (5)$$

gives a universal curve of normalized range in dimensionless units which can be approximated by expressions of the form

$$R_B = C\zeta^a \quad (6)$$

In the energy range around 1 keV, a close approximation to this function for CdS is[37]

$$R_B = 1.48\ \zeta^{1.29} \quad (7)$$

The maximum energy loss per unit depth occurs at a depth $U_o$ whose energy dependence has been fitted to the experimental measurements down to kV energies. Here[37]

$$U_o = 0.069\ \zeta^{1.71} \quad (8)$$

Similarly, $R_B$ has been fitted to the expression[37]

$$R_B = 0.62\ \zeta^{1.609} \quad (9)$$

over the same energy range. Hence, equations 7 and 9 apply to the same material over different energy ranges. The ratio of $U_o/R_B$ varies between different materials but appears to be constant for a specific material at different energies.[37] Thus from the $U_o/R_B$ ratio extracted from the fitted expressions at intermediate energy and Equation 7 at lower energies, we obtain an expression for $U_o$ at energies around 1kV equal to

$$U_o(E \leqq 1\ kV) = 0.1647\ \zeta^{1.392} \quad (10)$$

From these expressions, one can obtain the maximum energy range ($R_B'$) and the maximum of the depth-dose function ($U_o$) as a function of incident electron energy. For the semiconductors CdS, InP, and GaAs, I = 343. Between the kinetic energies of 500 and 5000 eV, $R_B$ varies from 15 nm to 300 nm, respectively while $U_o$ varies from 2 nm to 40nm, respectively. Hence at voltages of 500-1000 eV, the maximum energy loss occurs at depths which are orders of magnitude smaller than those of conventional high keV or MeV electron beams.

In order to analyze the intensity dependence of CLS features as a function of incident voltage, the incident beam current must be normalized to maintain a constant power dissipation over the depth range - to $R_B$ ($E \leqq$ 1kV) or to $U_o$ ($E \leqq$ 1kV). Thus over a 500 to 5000 eV voltage range, beam current must increase by a 1.95 {2.42} factor to maintain constant power dissipation over $R_B$ ($E \leqq$ 1kV) {$U_o$ ($E \leqq$ 1kV)}.

Comparison with experiment suggests that the energy dependence of the depth expressions is appropriate. Figure 2 illustrates the energy dependence of the near-band-edge luminescence of bulk InP (1.35 eV) along with two deep level transitions (0.8 eV and 1.0 eV) associated only with the surface (See Figure 4a).[48] Normalizing the 1.35 eV intensity at 1.0 kV to the maximum depth of energy loss $U_o$ (E = 1kV), one finds comparable increases for both at higher energies. Interestingly, the 1.35 eV CLS intensity increases ca.25% more slowly, in accordance with the maximum range rather than the depth of maximum energy loss. This may reflect the influence of the "dead layer," which is several hundred nm for this lightly n-doped InP crystal and whose electric field gradient gives more weight to CLS contributions from the deeper range.

The "surface" contributions associated with this system, 0.25 nm Au on InP (110), will be discussed in a later section. However, it is significant that surface and bulk peak intensities vary in a complementary way on the same depth scale as calculated for $U_o$ ($E \leqq$ 1kV). As a result, the depth of maximum excitation must not be blurred appreciably by the diffusion

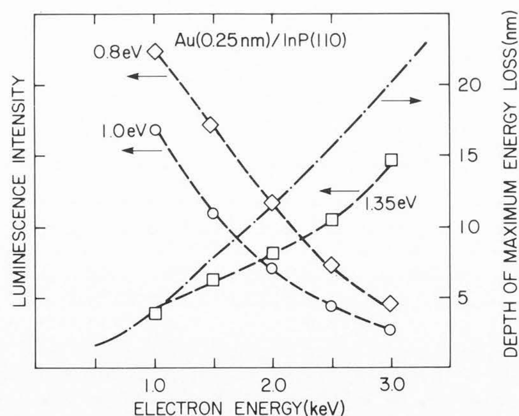


Fig. 2. Dependence of luminescence peak intensity and calculated excitation depth on incident electron energy for 0.8 eV, 1.0eV, and 1.35 eV features for 0.25 nm Au on n-type InP (110).

lengths of the cascading electrons, even though the latter can easily exceed micron distances. This effect may be due to n-type band bending in the surface space charge region which repels these secondary electrons.

## Cathodoluminescence Spectroscopy of Surface-Related States

Since the early 1970's, a number of researchers have used CLS to probe semiconductors. These investigations centered on $SiO_2$,[12,13,18] CdS,[25] GaAs[7,19,31,33,34], and ZnS[25]. Some work is also available for CdTe,[26] InP,[10] ZnO,[27,32] ZnSe,[14,40] Si[24] and diamond[54]. Norris et al.[25] were the first to emphasize the difference in electronic features between the semiconductor bulk and the region only a few hundred nm below the free surface. Such depth-dependent studies focussed primarily on changes in the near-surface region due to ion implantation and other damage effects. Wittry and Kyser's studies of GaAs band-edge luminescence versus incident energy[50] provided early evidence for the "dead layer" associated with band bending in the surface space charge region and indicated that the intensity of such luminescence could indeed serve as a gauge of the band bending voltage.

On the other hand, the intermediate energies of these early experiments hampered the observation of features associated with the outer few monolayers of semiconductors atoms. Likewise, the absence of UHV conditions and the use of polished and etched surfaces suggests that surface contamination and lattice damage were significant. Few if any electronic features of the clean, ordered surfaces are likely to survive under these conditions.[4]

More recent work makes use of single crystal cleavage under UHV conditions to obtain clean, ordered surfaces. Figure 3 illustrates the effect of metal adsorption on the cleaved InP (110) surface.[46,47] Prior to metallization, the UHV-cleaved surface exhibits no luminescence at energies below the near-band-edge transition. Upon addition of approximately one-half monolayer of various metals, each of these cases results in new emission deep within the InP band gap. Also shown are features associated with a stepped portion of a similar UHV-cleaved surface. High densities of broken bonds are expected for the stepped surface. The similarity between the various spectra suggests that metal deposition also produces broken bonds, at least with initial coverages.

For both metal adsorption and steps, the absolute intensity of near-band-edge emission decreases, consistent with an increase in band bending. Street et al.[39] have reported similar decreases of band edge emission for oxygen adsorption on UHV-cleaved InP.

Figure 3 demonstrates the surface sensitivity of the low energy CLS technique. These features are distinctly different from any sub-band gap features of the bulk semiconductor[41-43] which, if present, are observable with higher energy CLS as well as photoluminescence spectroscopy.

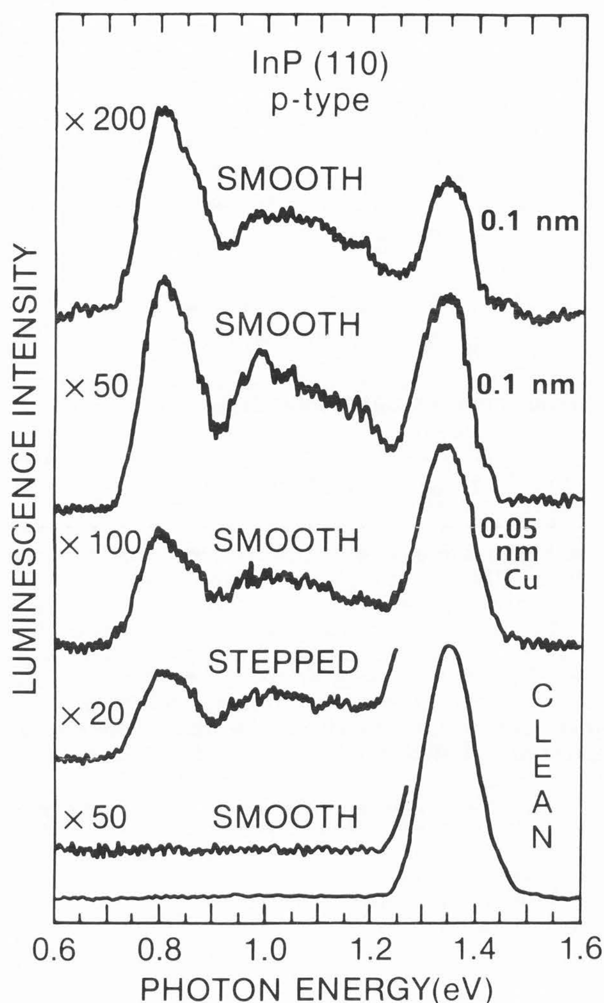


Fig. 3. Cathodoluminescence spectra obtained with 1.5 keV ($R_B = 60$ nm, $U_0 = 8$ nm) electrons of clean, mirror-like p-type InP (110) ($p = 10^{18}$ Zn-cm$^{-3}$) before and after submonolayer deposition of Ni, Pd, or Cu. The spectrum for the clean step-cleaved surface is shown for comparison.

## Cathodoluminescence Spectroscopy of Metal-Semiconductor Interface States

Low energy CLS is also sensitive to electronic states induced by chemical interactions at the metal-semiconductor substrate. These states and their evolution with coverage can differ significantly for various metals. Figure 4 illustrates the evolution of metal-induced states for the metals Au, Al, Cu, and Pd on InP.[46] New features induced by Au in Figure 4a extend from 0.8 eV to the band edge and evolve with coverage into a relatively narrow peak centered at 0.78eV. This spectral distribution diminishes rapidly between 0.8 and 0.7eV due to the corresponding drop in Ge detector response. However, compensation for the detector response does not alter the presence of the discrete peak feature.[48] Likewise, compensation for a narrow absorption

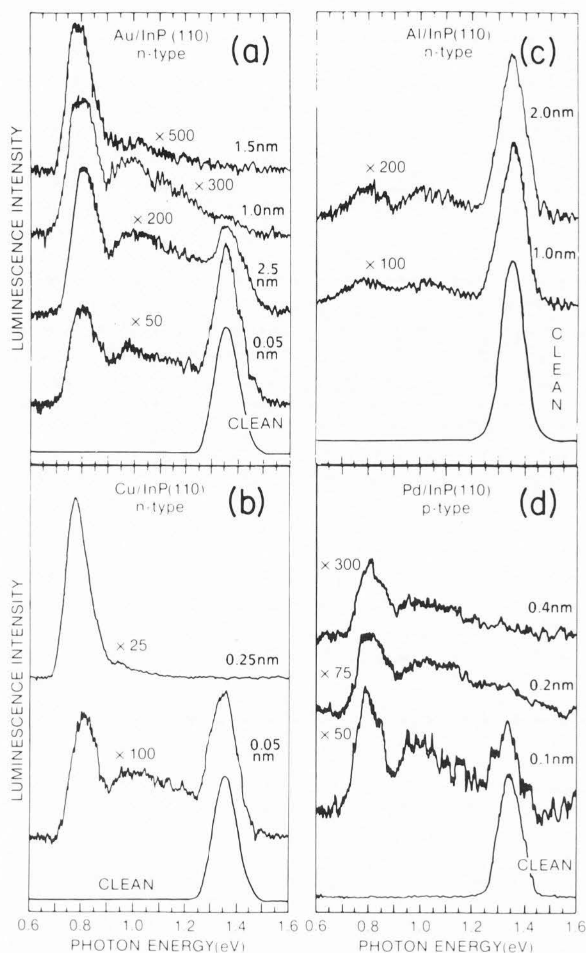


Fig. 4. Cathodoluminescence spectra obtained with 1.0 keV ($R_B = 40$ nm, $U_0 = 5$ nm) electrons of (a) Au, (b) Cu, and (c) Al on clean mirror-like n-type InP (110) ($n = 4.3 \times 10^{15}$ $cm^{-3}$ undoped), and (d) Pd on clean mirror-like p-type InP (110) ($p = 10^{18}$ Zn-$cm^{-3}$) as a function of increasing metal deposition.

band due to the quartz optics does not qualitatively change the appearance of the InP spectra in Figures 3-5.[48] Cu deposition also produces a large peak in the same region but at lower coverages and with a greater attenuation of the broad peak centered at 1.1 eV. Al and Pd coverages produce qualitatively different features with no pronounced mid-gap peak.

Evolution of these different CLS features with metal coverage and the corresponding decreases in near-band edge emission reflect the rate of band bending as measured by soft x-ray photoemission spectroscopy.[5] Furthermore the positions of the CLS peaks can account for the absolute band bending measured for the macroscopic metal-semiconductor contact.[46-48] Thus Figure 4 demonstrates that discrete interface-specific features evolve during the initial stages of Schottky barrier formation which, along with the magnitude of band bending, depend on the particular metal. These optical measurements are the first direct observations of metal-semiconductor interface states.

Metals can also induce changes in the recombination of charge carriers which depend on the surface morphology of the semiconductor coated by metal. For example, Al overlayers on smooth versus stepped portions of the same InP (110) surface exhibit a substantially different dependence of CLS intensities on electron injection level. For the smooth-cleaved surface, the relative amplitudes of features in Figure 4c are independent of beam

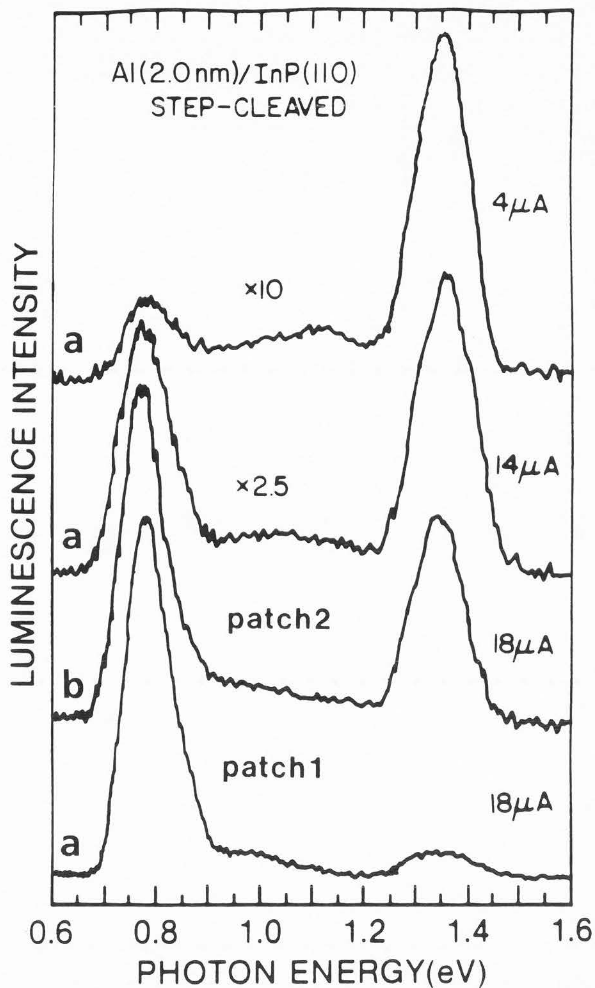


Fig. 5. Cathodoluminescence spectra obtained with 1.5 keV electrons of Al on step-cleaved n-type InP (110) ($n = 4.3 \times 10^{15}$ $cm^{-3}$ undoped) in ultrahigh vacuum for several incident beam currents at constant excitation depth. Spectra are normalized to maximum peak intensity. The 0.8 eV feature increases superlinearly with increasing injection level. Spectra for (a) and (b) correspond to different stepped patches of the same cleavage surface. The higher ratio of 1.35 eV versus 0.8 eV emission intensities for (b) versus (a) corresponds to a visually lower step density.

current over several orders of magnitude. Likewise, the step-cleaved surface without Al appears to be independent of beam current. However, for Al on the step-cleaved surface, one observes an increase in the 0.8 eV feature relative to the band edge emission and other features. Figure 5 illustrates the relative increase in the 0.8 eV feature with beam currents of 4 to 18μA (2 x $10^{17}$ - $10^{18}$ electrons/$cm^2$ - sec). These changes are reversible and therefore not due to any electron beam damage.[15,21] Such damage effects are negligible compared to those reported for high keV or MeV energies. Thermal effects are also small, as measured under comparable conditions earlier via the shift of the near-band-edge emission, whose energy increases with temperature.

The relative intensities of the midgap to near-band-edge features can vary between stepped areas and thus depends in part on the details of the step-cleaved surfaces. However, these variations occur only with metal deposition, implying an interaction between the metal and the step atoms. Since Al reacts with InP to form Al-P complexes which can self-limit the reaction,[3] the degree of step roughness could determine the penetration of the reaction beyond the atomic interface.

Figure 6 illustrates the injection level dependence of the these major CLS features for 2 nm Al on the stepped InP surface associated with Figure 5. The

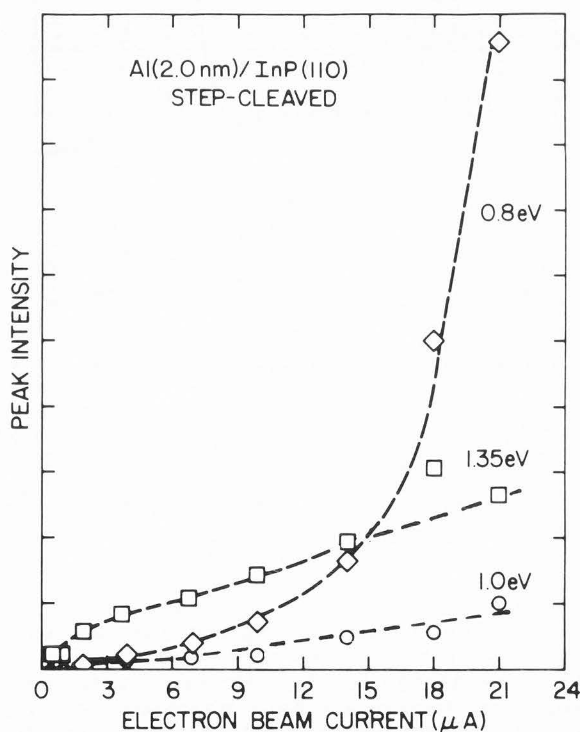


Fig. 6. Luminescence intensity for the 0.8 eV, 1.0 eV, and 1.35 eV peaks in Figure 5 versus injection current for step-cleaved InP with a 2 nm Al overlayer. The superlinear injection level dependence is absent for either Al-covered, smooth surfaces or for clean, step-cleaved surfaces.

1.0-1.1 eV and 1.35 eV peak intensities increase linearly with current over three orders of magnitude. In contrast the 0.8 eV level exhibits superlinear dependence which diverges at currents of only a few μA. This behavior is representative of radiative recombination with a density of mid-gap states (a) whose cross section depends nonlinearly on the density of free carriers (e.g., multiple-excited states) or (b) which is considerably higher than those for the higher energy transition or the band-to-band transition. In either case the metal / step states created in localized patches of the interface will produce trapping and recombination of free carriers which can be considerably different from the same transport characteristics of the smooth areas. Furthermore, the variation in absolute intensity of band edge emission from surface area to area indicates different band bending and therefore different Schottky barrier heights as well. Hence CLS provides evidence for nonuniformities in charge transport and rectification at metal-semiconductor junctions which depend sensitively on semiconductor surface morphology.

Bulk features of the semiconductor can also contribute to the sub-band gap CLS emission. These features typically appear for the clean surfaces and remain unchanged (albeit weaker) with metal coverages. An additional test for such bulk-related states is for one to compare CLS and photoluminescence spectroscopy features, since the latter can probe well beyond the surface space charge region.[20] As mentioned earlier, higher energy CLS can also provide evidence similar to that of photoluminescence. Preliminary results for different GaAs crystal surfaces reveals substantial mid-gap emission from the clean surface whose intensities vary considerably depending on dopant type and concentration as well as the method of crystal growth. Significantly, these widely varying results show little difference in gap state emission near the band edge, a region commonly used by researchers to assess the quality of crystal growth. The CLS observations of bulk crystal features suggests instead that mid-gap features are a much more appropriate figure of merit for assessing crystal quality.

### Cathodoluminescence of Interface Compounds and Defects via Pulsed Laser Annealing

CLS provides a measure of new compound band structure and/or deep level defects produced by thermal processing of "buried" metal-semiconductor interfaces. To promote such phenomena without substantial interdiffusion of chemical species, one can employ laser annealing with short (5 nsec pulsewidth) and high absorption (tens of nm for a 308nm excimer laser).[35,36] As an example, 5 nm Cu on CdS in Figure 7 induces a new feature at 1.28 eV which is enhanced by laser annealing.[6] The resultant peak feature corresponds closely to that of the compound $Cu_2S$.[11] On the other hand, Figure 8 illustrates the different CLS features produced by a 5 nm Al film on a similar CdS (1120) surface. Here laser annealing produces a pair of emission lines at 1.3 eV and 1.65 eV. The correspondence of the 1.65 eV structure with one of the bulk features observed by photoluminescence spectroscopy and the reduction of both 1.3 and 1.675 eV features with additional

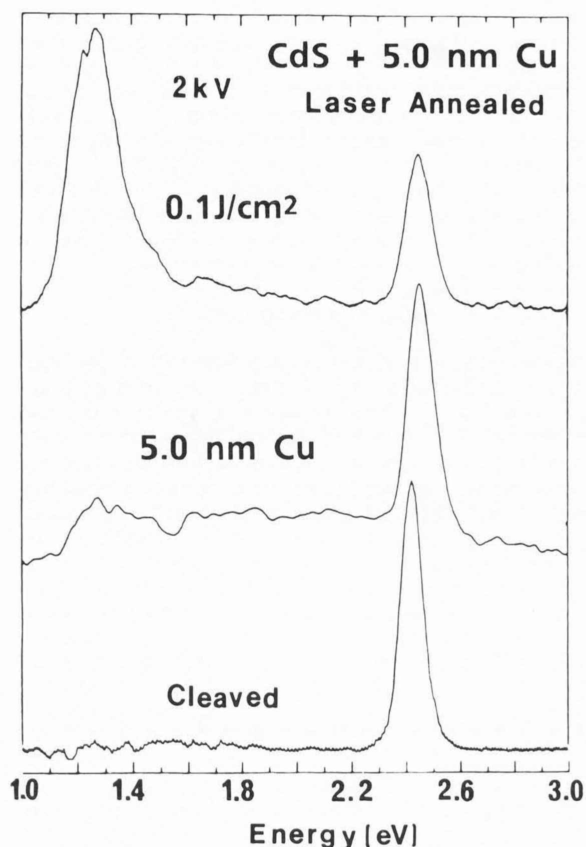


Fig. 7. Cathodoluminescence spectra obtained with 2keV electrons incident on UHV-cleaved CdS (1120) after deposition of 5 nm Al and after in-situ laser-annealing with energy density 0.1 J/cm$^2$.

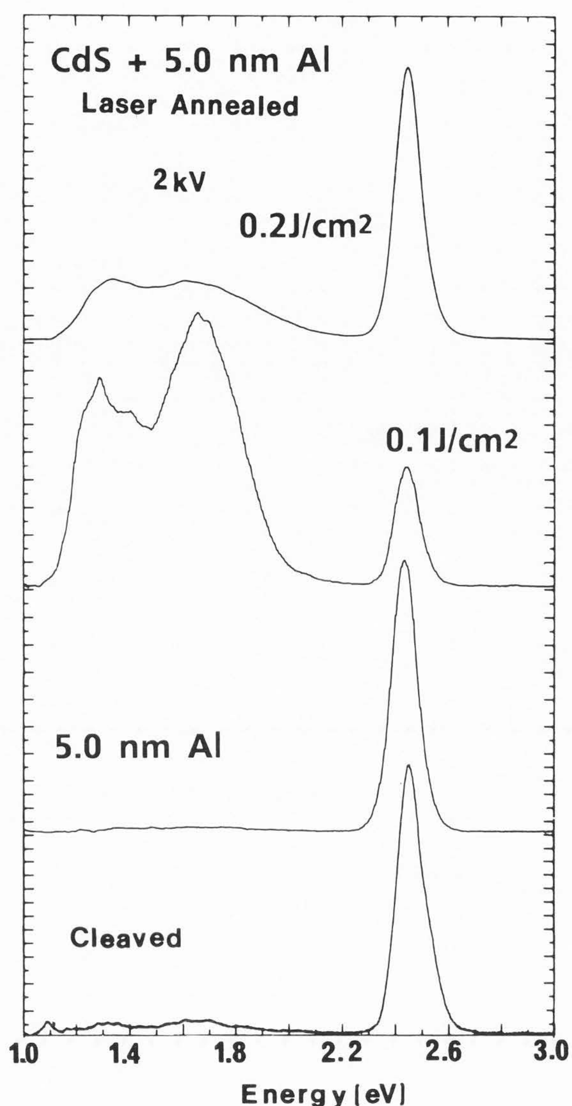


Fig. 8. Cathodoluminescence spectra obtained with 2kV electrons incident on UHV-cleaved CdS (1120) after deposition of 5 nm Al and after in-situ laser annealing with increasing energy density.

laser annealing suggests that both are due to lattice damage.

The incident energy dependence provides further information regarding the depth distribution of these damage-related peaks. In Figure 9a, the 2 keV (more bulk sensitive) spectrum exhibits relatively equal amplitudes for both deep level emissions whereas the 500 eV (more surface-sensitive) spectrum reveals a much larger 1.35 eV peak.[6] Thus the 1.35 eV emission state is located closer to the free surface within the top few tens of nm. This is consistent with melt depths of ca.20 nm for laser-induced reactions at the Al-InP interface.[36] In Figure 9b, the defect features at both incident energies decrease with respect to the near-band-edge emission, consistent with a reduction in their densities at higher annealing power levels.[6] Furthermore, comparison of 2 keV and 500 eV CLS spectra reveals little difference in amplitude between the two deep level peaks, indicating a more uniform spatial distribution of both states. Thus low energy CLS reveals that both metal interactions and their changes with thermal processing have major effects on electronic structure at the "buried" metal-semiconductor interface.

### Implications for Schottky Barrier Formation

Low energy CLS provides a powerful tool to examine electronic structure of metal-semiconductor interfaces. Besides probing at metal coverages well beyond the capabilities of more conventional surface science techniques, CLS provides information on band structure and deep levels which these other techniques cannot supply directly. In particular, CLS results have revealed that metals induced discrete interface states deep within the semiconductor band gap which correlate closely with the ultimate Fermi level position of the Schottky barrier.[46] These states evolve with different energies and at different rates of coverage for different metals. Such results support models of rectification which involve charge

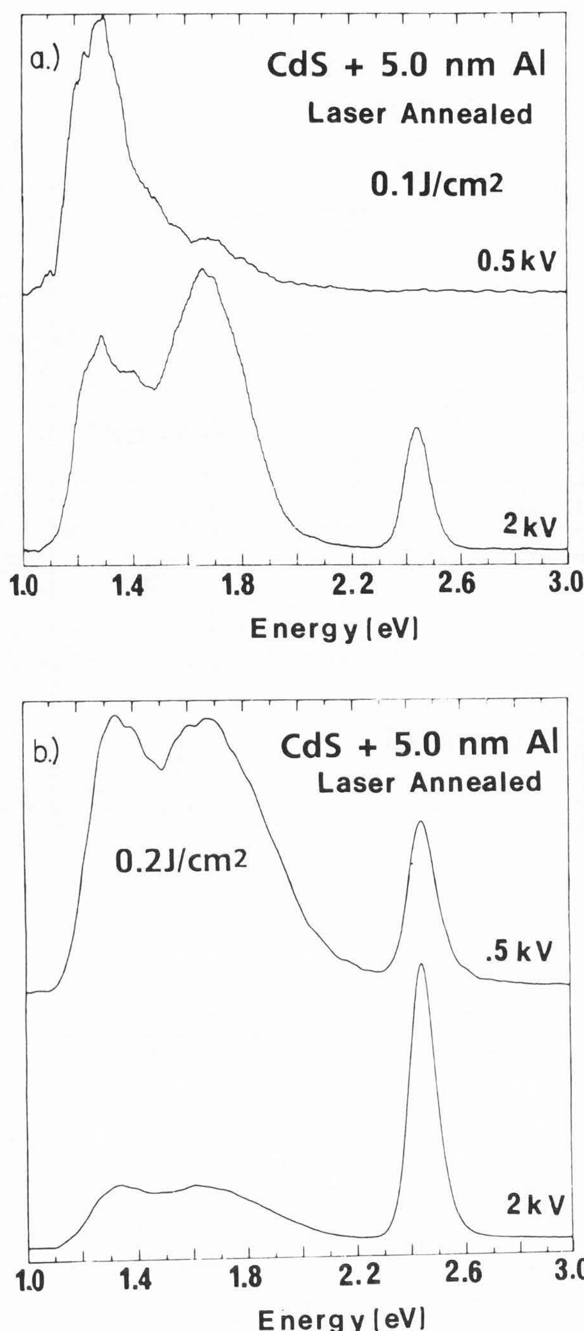


Fig. 9. Cathodoluminescence spectra as a function incident electron energy for UHV-cleaved CdS (1120) with a 5 nm Al overlayer, laser annealed with energy density (a) 0.1 J/cm$^2$ and (b) 0.2 J/cm$^2$.

transfer to localized states defined by the chemical interaction between metal and semiconductor.[1,2,4,9,16,52] They directly contradict models based on an absence of discrete states in the semiconductor band gap[44] as well as models which predict little or no differences for different metals.[38]

Further application of the CLS technique should refine our knowledge of these interface states, especially their chemical origin, their energy dependence on particular metals, their densities of states, and their trapping cross sections. CLS will also reveal to what extent bulk defects in some semiconductors influence the Fermi level stabilization at electrical contacts. Overall, CLS provides a direct probe of interface electronic phenomena which can play a major role in understanding Schottky barrier formation.

## Future Development

CLS research thus far has utilized a straight forward combination of electron gun and photon collection optics. The relative simplicity of the experimental technique lends itself to studies involving substantial in-situ specimen processing such as cleaning, metallization, and annealing. Nevertheless, detailed analysis of interfacial states requires more sophisticated measurements. For example, similar CLS experiments performed at cryogenic temperatures will enhance and sharpen the spectral features which, by comparison with reported photoluminescence features for known impurities and defects, may help identify the physical origin of the deep surface levels. The CLS dependence on injection current can provide evidence for differences in trapping cross sections and densities which are not otherwise apparent for different semiconductor surface morphologies. The time dependence of luminescence excitation and deexcitation (onset and decay times for emission following the respective start or end of electron bombardment) may allow one to extract capture cross sections, densities, and recombination lifetimes for these deep levels. Of course, this surface-enhanced technique can also provide surface maps of electronic structure as already performed for bulk levels via high energy cathodoluminescence or photoluminescence spectroscopies.[26,28-31,49] Likewise, the deep levels due to impurity diffusion could be used to establish bulk and surface diffusion constants for various adsorbates on semiconductor surfaces[40] once the energy depth-dose curve is properly fitted to a given overlayer-substrate material structure.

In conclusion, low energy CLS provides a host of information on the electronic structure of semiconductor interfaces which are difficult to obtain by other techniques. In the last few years, CLS results have demonstrated that the electronic properties of the "buried" interface are sensitive to the interaction between the contact materials and that these properties play a major role in Schottky barrier formation. With wider application and increased sophistication, the low energy CLS technique promises to reveal a host of detailed electronic information about semiconductor surfaces and interfaces.

## Acknowledgements

This work is supported in part by Office of Naval Research contract N00014-80-C-0778 (G. B. Wright).

## References


1. Brillson LJ. (1978). Transition in Schottky barrier formation with chemical reactivity. Phys. Rev. Lett. 40, 260-263.
2. Brillson LJ, Bachrach RZ, Bauer RS. (1979). Chemically-induced charge distribution at Al-GaAs interfaces. Phys. Rev. Lett. 42, 397-400.
3. Brillson LJ, Brucker CF, Katnani AD, Stoffel NG, Margaritondo G. (1981). Chemical basis for InP-metal Schottky barrier formation. Appl. Phys. Lett. 38, 784-786.
4. Brillson LJ. (1982). The structure and properties of metal-semiconductor interfaces. Surface Sci. Repts. 2, 123-326.
5. Brillson LJ, Brucker CF, Katnani AD, Stoffel NG, Daniels R, Margaritondo G. (1982). Fermi level pinning and chemical structure of InP-metal interfaces. J. Vac. Sci, Technol., 21, 564-568.
6. Brillson LJ, Richter HW, Slade ML, Weinstein BA, Shapira Y. (1985). Cathodoluminescence spectroscopy studies of laser-annealed metal-semiconductor interfaces. J. Vac. Sci. Technol. A3, 1011-1015.
7. Cone ML, Hengehold RL. (1983). Characterization of ion-implanted GaAs using cathodoluminescence. J. Appl. Phys. 54, 6346-6351.
8. Everhart TE, Hoff PH. ((1971). Determination of kilovolt energy dissipation versus penetration distance in solid materials. J. Appl. Phys.42, 5837.
9. Freeouf JL, Woodall JM. (1981). Schottky barriers: An effective work function model. Appl. Phys. Lett. 39, 727-729.
10. Gatos CH, Vaughan JJ, Lagowski J, Gatos HC. (1981). Cathodoluminescence of InP. J. Appl. Phys. 52, 1464-1469.
11. Guastavino F, Duchemin S, Rezig B, Grault B, Savelli M. (1978). Photon and electron excitation phenomena in copper sulfides. Conf. Rec. IEEE Photovoltaic Spec. Conf. Ser. 13, 303-308.
12. Koyama H, Matsubara K, Mauri M. (1977). Cathodoluminescence study of a silicon dioxide layer on silicon with the aid of Auger electron spectroscopy. J. Appl. Phys. 48, 5380-5381.
13. Koyama H. (1979). Cathodoluminescence study of $SiO_2$. J. Appl. Phys. 51, 2228-2235.
14. Krier A, Bryant FJ. (1986). Cathodoluminescence of laser-Annealed Erbium-implanted zinc selenide. J. Phys. Chem. Solids, 47, 719-725.
15. Lang DV. (1977). Review of radiation-induced defects in III-V compounds. Inst. Phys. Conf. Ser. 31, 70-94.
16. Ludeke R, Landgren G. (1986). Electronic properties and chemistry of Ti/GaAs and Pd/GaAs interfaces. Phys. Rev. B33, 5526-5535.
17. Magnea N, Petroff PM, Capasso F, Logan RA, Alva K, Cho AY. (1985). Electric field dependence cathodoluminescence of III-V compound heterostructures: A new interface characterization technique. Appl. Phys. Lett. 46, 1074-1076.
18. McKnight SW, Palik ED. (1980). Cathodoluminescence of $SiO_2$ films. J. Noncrystalline Solids 40, 595-603.
19. McKnight SW, Palik ED, Bhar TN, (1980). Cathodoluminescence studies of anodic oxides on GaAs. J. Vac. Sci. Technol. 17, 967-970.
20. Mettler K. (1977). Photoluminescence as a tool for the study of the electronic surface properties of gallium arsenide. Appl. Phys. 12, 75-82.
21. Mircea A, Bois D. (1979). A review of deep-level defects in III-V semiconductors. Inst. Phys. Conf. Ser. 46, 82-99.
22. Murata K. (1976). Exit angle dependence of penetration depth of backscattered electrons in the scanning electron microscope. Phys. Stat. Sol. (a) 36, 197-208.
23. Murata K. (1976). Depth resolution of the low- and high-deflection backscattering electron images in the scanning electron microscope. Phys. Stat. Sol. (a) 36, 527-532.
24. Myhajlenko S, Ke W, Hamilton B. (1983). Cathodoluminescence assessment of electron beam recrystallized silicon. J. Appl. Phys. 54, 862-867.
25. Norris CB, Barnes CE, Beezhold W. (1973). Depth-resolved cathodoluminescence in undamaged and ion-implanted GaAs, ZnS, and CdS. J. Appl. Phys. 44, 3200-3221.
26. Norris CB, Barnes CE, Zanio KR. (1977). Cathodoluminescence studies of anomalous ion implantation defect introduction in CdTe. J. Appl. Phys. 48, 1659-1667.
27. Paqlueras J, Kubalek E. (1985). Cathodoluminescence from deformed ZnO ceramics. Solid State Commun. 54, 745-746.
28. Petroff PM, Lang DV, Strudel JL, Logan RA. (1978). Scanning transmission electron microscopy techniques for simultaneous electronic analysis and observation of defects in semiconductors. Scanning Electron Microsc. 1978; I:325-332.
29. Petroff PM, Lang DV, Logan RA, Strudel JL, (1980). Analyzing semiconductor defects. Circuits Manufacturing 4, 35-54.
30. Petroff PM, Miller RC, Gossard AC, Weigmann W. (1984). Impurity trapping, interface structure, and luminescence of GaAs quantum wells grown by molecular beam epitaxy. Appl. Phys. Lett. 44, 217-219.
31. Petroff PM. (1985). Defects in III-V compound semiconductors in semiconductors and semimetals, Vol. 22A, (Eds.) Willardson RK and Beer AC. (Academic Press, New York) 379-403.
32. Pierce BJ, Hengehold RL. (1976). Depth-resolved cathodoluminescence of ion-implanted layers in zinc oxide. J. Appl. Phys. 47, 644-651.
33. Rakshit S, Biswas SN, Chakravarti AN. (1971). Dependence of the intensity of spontaneous emission from electron-beam-excited specimens of impure GaAs on the level of excitation. Phys. Stat. Sol. (a) 7, 593-595.
34. Rao-Sahib TS, Wittry DB. (1969). Measurement of diffusion lengths in p-type gallium arsenide by electron beam excitation. J. Appl. Phys. 40, 3745-3750.
35. Richter H, Brillson LJ, Daniels RR, Kelly M, Margaritondo G. (1984). Control and characterization of metal-InP and GaAs interfaces formed by laser-enhanced reactions. J. Vac. Sci. Technol. B2, 591-596.
36. Richter HW, Brillson LJ, Kelly MK, Daniels RR, Margaritondo G. (1986). Laser-induced chemical reactions at the Al / III-V compound semiconductor interface. J. Appl. Phys. 60, 1994-2002.
37. Shea SP. (1984). Energy and atomic number dependence of electron depth-dose and lateral-dose functions, in: Electron Beam Interactions With Solids, D.F.Kyser, D.E.Newbury, H. Niedrig, R. Shimizu (eds), SEM, Inc., AMF O'Hare, IL 60666, 145-151: and references therein.

38. Spicer WE, Lindau I, Skeath P, Su CY. (1980). Unified defect model and beyond. J. Vac. Sci. Technol. 17, 1019-1027.
39. Street RA, Williams RH, Bauer RS. (1980). Influence of the surface on photoluminescence from indium phosphide crystals. J. Vac. Sci. Technol. 17, 1001-1004.
40. Takenoshita H, Kodo K, Sawai K. (1986). Cathodoluminescence study of diffusion coefficients of Al, Ga, and In in ZnSe. Jpn, J. Appl. Phys. 25, 1610-1611.
41. Tempkin H, Bonner WA. (1981). Photoluminescence study of melt grown InP. J. Appl. Phys 52, 397-401.
42. Tempkin H, Dutt BV, Bonner WA. (1981). Photoluminescence study of native defects in InP. Appl. Phys. Lett. 38, 431-433.
43. Tempkin H, Dutt BV, Bonner WA, Keramidas VG. (1982). Deep radiative levels for InP. J. Appl. Phys. 53, 7526-7533.
44. Tersoff J. (1985). Schottky barriers and semiconductor band structures. Phys. Rev. B32, 6968-6971.
45. Vilms J, Spicer WE. (1965). Quantum efficiency and radiative lifetime in p-type gallium arsenide. J. Appl. Phys. 36, 2815-2821.
46. Viturro RE, Slade ML, Brillson LJ. (1986). Optical-emission properties of interface states for metals in III-V compounds. Phys. Rev. Lett. 57, 487-490.
47. Viturro RE, Slade ML, Brillson LJ. (1977). Cathodoluminescence spectroscopy of metal/III-V semiconductor interface states. Proc. 18th International Conference on the Physics of Semiconductors, (Ed.) Engström O. (World Scientific Publishing Co. Pte Ltd., Singapore, 1977), 371-374.
48. Viturro RE, Slade ML, Brillson LJ. (1988). Optical emission properties of metal/InP and GaAs interface states. J. Vac. Sci. Technol., in press.
49. Warwick CA, Brown GT. (1985). Spatial distribution of 0.68 eV emission from undoped semi-insulating gallium arsenide revealed by high resolution luminescence imaging. Appl. Phys. Lett. 46, 574-576.
50. Wittry DB, Kyser DF. (1967). Measurements of diffusion lengths in direct gap semiconductors by electron-beam excitation. J. Appl. Phys. 38, 375-382.
51. Wittry DB. (1984). Gaussian models for the energy distribution of excitation in solids: Applications to x-ray microanalysis and solid state electronics. Scanning Electron Microsc. 1984; I:99-108.
52. Woodall JM, Freeouf JL. (1981). GaAs metallization: some problems and trends. J. Vac. Sci. Technol. 19, 794-798.
53. Yacobi BG, Holt DB. (1986). Cathodoluminescence scanning electron microscopy of semiconductors. J. Appl. Phys. 59, R1-R24.
54. Yamamoto N, Spence JCH, Fathy D. (1984). Cathodoluminescence and polarization studies from individual dislocations in diamond. Phil. Mag. B49, 609-629.

## Discussion With Reviewers

**S. Myhajlenko**: Even though very low beam voltages (low penetration) have been used, is the spatial (depth) resolution of the CLS measurement not limited by carrier diffusion? This may be a micron or so for InP at room temperature.

**Authors**: Carrier diffusion can actually increase rather than decrease the surface sensitivity. The random scattering of excited electrons and the diffusion of thermal carriers at depths of only a few tens of nm will result in an accumulation of electron - hole pairs near the surface (over and above any band bending effects). With increasing distance from the surface, such accumulation decreases as the excitation depth increases toward or exceeds the thermal carrier diffusion length. Carrier diffusion is expected to reduce the depth discrimination. However, the pronounced voltage dependence of the CLS spectra presented here suggests that extended diffusion of thermal carriers does not make a dominant contribution to the radiative recombination.

**S. Myhajlenko**: If the recombination is 'pinned' in the surface depletion region, then the excess carriers would lead to a redistribution of the 'equilibrium' space charge, leading to a change in the band bending, which would affect the band edge CL. This would lead to a non-linear dependence of CL with excitation. This was not observed (fig. 6) - any comments?

**Authors**: With the injection levels indicated in Figure 6 and neglecting losses due to reflection as well as lateral diffusion, we estimate our volume carrier generation to be ca. $10^{23}$-$10^{25}$ electron-hole pairs-$cm^{-3}$ for the excitation energies and depths discussed in the paper. Assuming a carrier lifetime of $10^{-9}$ sec, this means excess minority carrier concentrations of $10^{14}$ - $10^{16}$ $cm^{-3}$ versus bulk carrier concentrations of $5x10^{15}$ -$10^{18}$ $cm^{-3}$. Furthermore, only a fraction of minority carriers generated reach the surface and compensate the space charge. Thus the excess carriers may not affect the band bending significantly at these concentrations. Nevertheless, the point is well taken and we plan to explore the effect of excess free carriers on the surface band bending.

**S. Myhajlenko**: The authors say that variation in band edge emission from surface area to area indicates different band bending and therefore different Schottky barrier heights. What is the spatial resolution of the CLS apparatus?

**Authors**: The spatial resolution of the CLS apparatus is defined by the spot size of the electron beam. In our case, the glancing incidence beam had a nominal diameter of a fraction of a millimeter. Of course, the technique can be extended to much higher resolution.

**S. Myhajlenko**: Could this variation be mapped by EBIC?

**Authors**: Yes, we have indeed used EBIC to map these variations. The corresponding displayed image shows darker and lighter areas that can be assigned to differences in band bending.

**S. Myhajlenko:** Or have the authors measured this variation in barrier height directly by electron beam induced voltage (EBIV)?
**Authors:** No, we haven't. However, this should certainly be possible to do with this technique.

**R. L. Hengehold:** How do the results obtained from low energy CLS compare with those from photoluminescence using excitation from a short wavelength (ca. 350nm) laser?
**Authors:** Initial studies of photoluminescence from semiconductors using a 5 mw He-Cd (442nm) laser suggest much lower intensities from surface features relative to the CLS results described in this paper. Furthermore, only a small variation in the depth of excitation is possible (by varying the angle of incidence of the laser with the specimen surface).

**R. L. Hengehold:** Is it possible to obtain depth resolved information on the surface by either varying the beam energy or the thickness of the metal overcoat? How would the spectra be deconvolved in this case?
**Authors:** Increasing the thickness of the metal overcoat decreases the energy of electrons penetrating to the semiconductor surface, thereby enhancing the excitation at the interface. In this sense, overcoat thickness and electron beam energy are complementary. However, thicknesses above a few nanometers are necessary to have a significant effect on the excitation depth and such thicknesses will in general attenuate significantly the luminescence signal passing back through the metal. In order to overcome this problem, one can in principle collect the light emitted by deep level transitions through the opposite side of the semiconductor.

With a metal overlayer on a semiconductor, deconvolution of the spectral features is trivial since only the semiconductor contributes to the emission. For one semiconductor layer on another (e.g., a heterojunction), we have unpublished data showing relative intensities consistent with the excitation depths derived in this paper. In order to determine the depth-dose function in both layers, one must take into account the different atomic weight, number, and density of the overlayer versus the substrate. To lowest order approximation, the excitation depth in the substrate decreases by the thickness of the overlayer. A comparison of depth-dose functions for the two materials with the same incident energies would provide an additional weighting factor for the overlayer thickness. Alternatively, the change in atomic weight, number, and density could be incorporated explicitly into a Monte Carlo calculation with appropriate boundary conditions. (See following question.) Note that band bending and carrier diffusion will contribute to the relative intensities of two optically-active materials as well.

**D. B. Holt:** Have you tried using Monte Carlo simulations to obtain information on the excitation at various depths for different materials and beam voltages? (For a good introductory account and microcomputer program see: e.g. Chapt. 1 in D. E. Newbury, D. C. Joy, P. Echlin, C. E. Fiori and J. I. Goldstein, Advanced SEM and X-ray Microanalysis (Plenum) 1986.) Such depth-dose functions can quickly be obtained for particular specimen geometries (metal layer thickness and semiconductor substrate), beam tilts and voltages with modern microcomputers using basic physical (scattering) parameters. Have you any comments on the applicability of this approach to your extreme values of some of the geometrical parameters?
**Authors:** We are planning to compare the depth-dose functions obtained by this Monte Carlo program with the functions calculated by the analysis given in this paper. Computer-generated figures of the former appear to be in qualitative agreement with the latter at the lowest energies (5 keV) shown. We are particularly interested in evaluating the effect of our oblique beam tilts and overlayer film thicknesses. Because of the extremely thin metal coverages used in our experiments, the overlayers may not be uniform. Such nonuniform morphology will reflect itself in the comparison of observed versus calculated excitation depth as a function of metal thickness and beam energy.

**D. B. Holt:** Your demonstration that it is possible to observe and separate out surface states is very important. How difficult is it experimentally? Is the problem of low intensities not severe and how do you overcome this? Do you use high power "flood" bombardment? What would happen if ultra-high vacuum were not employed so "real world" contacts were more closely approximated?
**Authors:** The detection of luminescence from surface state transitions is relatively difficult, due to the extremely thin layer of material involved. Nevertheless, several physical factors aid detection, i.e., the relatively high level of excitation near the surface, diffusion of carriers excited below the surface to surface recombination sites, and decreased luminescence intensity from the surface space charge region due to band bending. In practice, a high-detectivity photodetector and lock-in detection can make a major difference in observing such signals. We do not use high power "flood" bombardment. Beam currents are usually restricted to a few microamps over a $10^{-2}$-$10^{-4}$ $cm^2$ surface area in order to minimize heating. The electron beam is confined to the focal area of the monochromator. Without UHV conditions, one expects a strong perturbation of the energies and densities of the surface states due to ambient chemisorption. However, subsurface features may not be as strongly affected.

**D. B. Holt:** In the case of the difference between stepped and smooth InP spectra, is there any possibility of obtaining sufficient spectral and spatial resolution to be able to image steps directly? It is possible that the stepped surface states are localized at kinks along steps. In that case, non-uniform step contrast might be observed, distinguishing heavily kinked lengths of step from crystallographically-aligned segments.
**Authors:** The superlinear intensity behavior of sub-band gap features found for stepped versus smooth InP surfaces suggests a method of highlighting step features simply by modulating beam current density. While images with spatial resolutions of ca. 10 nm are achievable with low energy electron beams (see, for example, W. Telieps and E. Bauer, Surface Sci. **162**, 163 (1987)), they will be degraded by the electron cascade and free carrier diffusion.